14

Numerical Simulation of Solar Cells and Solar Cell Characterization Methods: the Open-Source on Demand Program AFORS-HET

Rolf Stangl, Caspar Leendertz and Jan Haschke
Helmholtz-Zentrum Berlin für Materialien und Energie, Institut für Silizium Photovoltaik, Kekule-Str.5, D-12489 Berlin Germany

1. Introduction

Within this chapter, the principles of numerical solar cell simulation are described, using AFORS-HET (**a**utomat **for** **s**imulation of **het**erostructures). AFORS-HET is a one dimensional numerical computer program for modelling multi layer homo- or heterojunction solar cells as well as some common solar cell characterization methods.
Solar cell simulation subdivides into two parts: optical and electrical simulation. By optical simulation the local generation rate $G(\mathbf{x},t)$ within the solar cell is calculated, that is the number of excess carriers (electrons and holes) that are created per second and per unit volume at the time t at the position $\mathbf{x}$ within the solar cell due to light absorption. Depending on the optical model chosen for the simulation, effects like external or internal reflections, coherent superposition of the propagating light or light scattering at internal surfaces can be considered. By electrical simulation the local electron and hole particle densities $n(\mathbf{x},t), p(\mathbf{x},t)$ and the local electric potential $\varphi(\mathbf{x},t)$ within the solar cell are calculated, while the solar cell is operated under a specified condition (for example operated under open-circuit conditions or at a specified external cell voltage). From that, all other internal cell quantities, such like band diagrams, local recombination rates, local cell currents and local phase shifts can be calculated. In order to perform an electrical simulation, (1) the local generation rate $G(\mathbf{x},t)$ has to be specified, that is, an optical simulation has to be done, (2) the local recombination rate $R(\mathbf{x},t)$ has to be explicitly stated in terms of the unknown variables n, p, φ , $R(\mathbf{x},t) = f(n, p, \varphi)$. This is a recombination model has to be chosen. Depending on the recombination model chosen for the simulation, effects like direct band to band recombination (radiative recombination), indirect band to band recombination (Auger recombination) or recombination via defects (Shockley-Read-Hall recombination, dangling-bond recombination) can be considered.
In order to simulate a real measurement, the optical and electrical simulations are repeatedly calculated while changing a boundary condition of the problem, which is specific to the measurement. For example, the simulation of a i-V characteristic of a solar cell is done by calculating the internal electron and hole current (the sum of which is the total current) as a function of the externally applied voltage.

Source: Solar Energy, Book edited by: Radu D. Rugescu,
ISBN 978-953-307-052-0, pp. 432, February 2010, INTECH, Croatia, downloaded from SCIYO.COM

Most solar cells, which are on the market today, can be described as a one dimensional sequence of different semiconductor layers. If they are uniformly illuminated, a one dimensional solar cell modelling is sufficient (the internal electron/hole current can flow only in one direction). This is the case for most wafer based silicon solar cells as well as for most thin film solar cells on glass as long as the integrated series connection shall not be explicitly modelled, see Fig.1 (left).

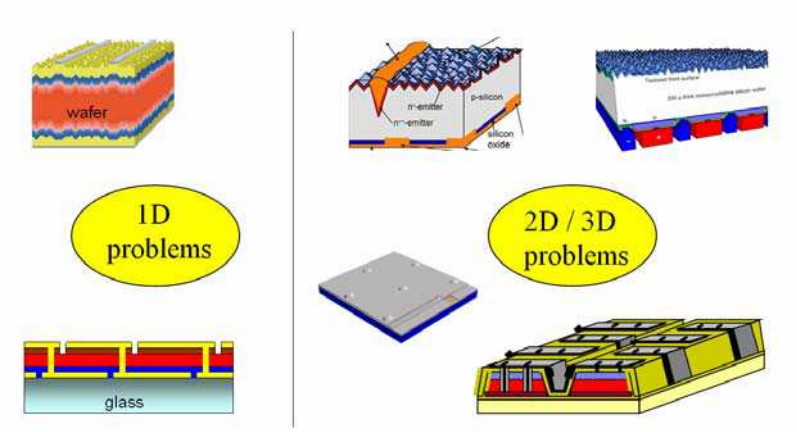

Fig. 1. solar cell structures which can be treated as a one dimensional problem (left), or which have to be treated as a two or even three dimensional problem (right).

However, in order to minimize contact recombination, stripe- or point-like metallic contacts which are embedded within an insulating passivation layer (i.e. silicon nitride, silicon oxide) are sometimes introduced. These contacts can either be placed on both sides of the solar cell or favourably only at the rear side of the solar cell, thereby avoiding shadowing due to the contacts. In these cases, the resulting solar cells have to be modelled as two or even three dimensional problems (the internal electron/hole current can flow in 2 or even 3 directions), see Fig.1 (right). In the current version 2.4 of AFORS-HET only 1D simulations are possible; however, there is a 2D mode under development.

Another possibility to reduce contact recombination is the use of heterojunctions, that is different semiconductors are used to form the solar cell absorber (photon collecting area), the electron extracting area and the hole extracting area of the solar cell. Ideally, the excess carriers of the solar cell absorber (electrons and holes) should be selectively attracted/repelled towards the contacts, see Fig. 2. These selective contacts can be either conventionally realized by doping/counter doping of the solar cell absorber, leading to a formation of an internal electric field by which the selective excess carrier separation is achieved. In this case, homojunctions will form, i.e. there are no band offsets, as the absorber and the electron/hole extracting areas of the solar cell consist of the same semiconductor. In principle, if different semiconductors with appropriately matched work functions are used to form the electron/hole extracting areas, heterojunctions can be formed having the same internal electric field as the homojunction, but with additional band offsets that enhance the repelling character of the contacts, see Fig. 2 (right).

A heterojunction solar cell will thus have a higher open circuit voltage compared to a homojunction solar cell. Less excess carriers of the repelled type are transported into the

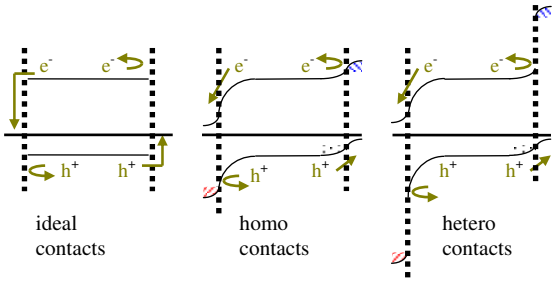

Fig. 2. schematic sketch of selective absorber contacts (band diagrams of a p-type semiconductor used as an absorber material). Ideal contacts (left), homojunction contacts (middle) and ideally aligned heterojunction contacts (right). NOTE: The dimensions of the x axis are schematic and not in scale!

electron/hole collecting regions, and thus the contact recombination at the metallic contacts is reduced. However, an essential pre-requisite is not to create too many interface defects during the formation of the heterojunction at the interface between the absorber and the electron/hole collecting area, which will otherwise act as additional recombination centres.

A realistic computer program for solar cell modelling should therefore be able to handle homojunctions as well as heterojunctions, and it should be able to consider interface defects and the corresponding interface recombination $R^{it}(t)$. Depending on the physical assumption how to describe an electron/hole transport across a heterojunction interface, a distinct interface model has to be chosen. For example, within the current version of AFORS-HET 2.4 a drift-diffusion and a thermionic emission interface model can be chosen, allowing the placement of interface defects but neglecting tunnelling. Tunneling interface models are under development.

To assure a numerical simulation with reliable results, a good model calibration, i.e. a comparison of simulation results to a variety of different characterisation methods, is necessary. The solar cell under different operation conditions should be compared to the simulations. Also different characterisation methods for the solar cell components, i.e. for the individual semiconductor layers and for any sub stacks should be tested against simulation. Only then the adequate physical models as well as the corresponding model input parameters can be satisfactory chosen. Thus a good solar cell simulation program should be able to simulate the common characterisation methods for solar cells and its components.

In this chapter, we describe AFORS-HET (**a**utomat **for s**imulation of **het**erostructures), a one dimensional numerical computer program to simulate solar cells as well as typical solar cell characterisation methods. Thus a variety of different measurements on solar cell components or on the whole solar cell can be compared to the corresponding simulated measurements in order to calibrate the parameters used in the simulations.

All optical and electrical models, which can be used in AFORS-HET, are discussed and their mathematical and physical background is stated. Furthermore, many solar cell characterisation methods, which can be simulated by AFORS-HET, are sketched. The difference in modelling thick film (wafer based) or thin film solar cells on glass will be investigated in order to choose the appropriate model. The basic input parameters of the corresponding models are described. Some selected results in modelling wafer based amorphous/crystalline silicon solar cells illustrate the concepts of numerical solar cell simulation within practical applications.

2. Brief description of AFORS-HET

The current version 2.4 of AFORS-HET solves the one dimensional semiconductor equations (Poisson´s equation and the transport and continuity equation for electrons and holes) with the help of finite differences under different conditions, i.e.: (a) equilibrium mode (b) steady state mode, (c) steady state mode with small additional sinusoidal perturbations, (d) simple transient mode, that is switching external quantities instantaneously on/off, (e) general transient mode, that is allowing for an arbitrary change of external quantities. A multitude of different physical models has been implemented. The generation of electron/hole pairs (optical models of AFORS-HET) can be described either by Lambert-Beer absorption including rough surfaces and using measured reflection and transmission files, or by calculating the plain surface incoherent/coherent multiple internal reflections, using the complex indices of reflection for the individual layers. Different recombination models can be considered within AFORS-HET: radiative recombination, Auger recombination, Shockley-Read-Hall and/or dangling-bond recombination with arbitrarily distributed defect states within the bandgap. Super-bandgap as well as sub-bandgap generation/recombination can be treated. The following interface models for treating heterojunctions are implemented: Interface currents can be modelled to be either driven by drift diffusion or by thermionic emission. A band to trap tunnelling contribution across a hetero-interface can be considered. The following boundary models can be chosen: The metallic contacts can be modelled as flatband or Schottky like metal/semiconductor contacts, or as metal/insulator/semiconductor contacts. Furthermore, insulating boundary contacts can also be chosen.
Thus, all internal cell quantities, such as band diagrams, quasi Fermi energies, local generation/recombination rates, carrier densities, cell currents and phase shifts can be calculated. Furthermore, a variety of solar cell characterisation methods can be simulated, i.e.: current voltage, quantum efficiency, transient or quasi-steady-state photo conductance, transient or quasi-steady-state surface photovoltage, spectral resolved steady-state or transient photo- and electro-luminescence, impedance/admittance, capacitance-voltage, capacitance-temperature and capacitance-frequency spectroscopy and electrical detected magnetic resonance. The program allows for arbitrary parameter variations and multidimensional parameter fitting in order to match simulated measurements to real measurements.
AFORS-HET, version 2.4, is an open source on demand program. If you want to contribute send an e-mail to AFORS-HET@helmholtz-berlin.de, specifying in detail what you would like to implement. It is distributed free of charge and it can be downloaded via internet:

http://www.helmholtz-berlin.de/forschung/enma/si-pv/projekte/asicsi/afors-het/index_en.html

3. Basic input parameter of AFORS-HET and associated physical models

3.1 Optical parameter (super bandgap generation optical models)

The incoming spectral photon flux $\Phi_0(\lambda,t)$, that is the number of incident photons of wavelength λ at the time t, has to be stated. In order to calculate the local super-bandgap generation rate $G(x,t)$ within the semiconductor stack, that is the number electrons and holes that are created per second and per unit volume at the time t at the position x due to super-bandgap light absorption, there are two optical models available: (1) Lambert-Beer absorption and (2) coherent/incoherent internal multiple reflections. For both models, the thicknesses L_i and the dielectric properties of the semiconductor layers have to be specified,

i.e. the complex refractive indices, $\tilde{n}_i(\lambda) = n_i(\lambda) - \mathrm{i}\, k_i(\lambda)$ with refractive index $n(\lambda)$ and extinction coefficient $k(\lambda)$. If the model Lambert-Beer absorption is chosen, a measured reflectivity $R(\lambda)$ of the semiconductor stack can be specified, and the resulting absorption $A(\lambda, x, t)$ within the semiconductor stack will be calculated, assuming Lambert Beer absorption by using the specified values for $k_i(\lambda)$ only and performing a ray tracing in order to account for textured surfaces and multiple bouncing of the radiation within the stack. If the model coherent/incoherent internal multiple reflections is chosen, the reflectivity $R(\lambda)$, the transmisivity $T(\lambda)$ and the absorption $A(\lambda, x, t)$ of the semiconductor stack is calculated from the specified values $n_i(\lambda)$, $k_i(\lambda)$, assuming plain surfaces within the stack but taking coherent internal multiple reflections into account, if desired. For both models, $G(x,t)$ is calculated from $A(\lambda, x, t)$ by integration over all wavelengths of the incident spectrum. In order to model optical sub-bandgap generation, optical electron/hole capture cross sections $\sigma_{n,opt} \neq 0$, $\sigma_{p,opt} \neq 0$ for the Shockley-Read-Hall defects have to be specified.

3.2 Layer parameter (semiconductor bulk models)

For each semiconductor layer, the thickness L, the electron/hole mobilities μ_n, μ_p, the effective valence/conduction band densities N_V, N_C, the electron/hole thermal velocities v_n, v_p, the electron affinity χ, the relative dielectric constant ε, the doping profile $N_D(x)$, $N_A(x)$ and the bandgap E_g of the semiconductor has to be specified. In order to describe recombination within the semiconductor, up to four different recombination models can be chosen, (1) radiative recombination, (2) Auger recombination, (3) Shockley-Read-Hall recombination, (4) dangling bond recombination. For radiative recombination, the radiative band to band rate constant r^{bb} has to be specified (Sze & Kwok, 2007). For Auger recombination, the electron/hole Auger rate constants r_n^{Aug}, r_p^{Aug} have to be specified (Sze & Kwok, 2007). For Shockley-Read-Hall recombination, the defect density distribution within the bandgap of the semiconductor $N_{trap}(E)$ and two capture cross sections σ_n, σ_p and if needed also two optical capture cross sections σ_n^{opt}, σ_p^{opt} for the electron/hole capture have to be specified (Sze & Kwok, 2007). For dangling bond recombination, the defect distribution within the bandgap of the semiconductor $N_{trap}(E)$, four capture cross sections σ_n^+, σ_p^0, σ_n^0, σ_p^- and the correlation energy U have to be specified (Sah & Shockley, 1958). Optical capture is not yet implemented in case of dangling bond recombination.

3.3 Interface parameter (semiconductor/semiconductor interface models)

The electron/hole current transport across a semiconductor/semiconductor interface can be described by three different interface models, (1) no interface, (2) drift diffusion interface, (3) thermionic emission interface. If no interface is chosen, no additional interface defects can be specified. Otherwise, an interface defect distribution $N_{trap}^{it}(E)$ can be specified. If the drift diffusion interface is chosen, an interface thickness L_{it} and interface capture cross sections σ_n^{it}, σ_p^{it} have to be specified. For both models (1) and (2), transport across the semiconductor/semiconductor interface is treated according to the drift-diffusion approximation like in the bulk of the semiconductor layers (Sze & Kwok, 2007). If the thermionic emission interface is chosen, the interface is regarded to be infinitively thin and

four capture cross sections $\sigma_{n,I}^{it}$, $\sigma_{n,II}^{it}$, $\sigma_{p,I}^{it}$, $\sigma_{p,II}^{it}$ and if needed also four optical capture cross sections $\sigma_{n,I}^{it,opt}$, $\sigma_{n,II}^{it,opt}$, $\sigma_{p,I}^{it,opt}$, $\sigma_{p,II}^{it,opt}$ for electron/hole capture from both sides of the interface have to be specified. Transport across the interface is then treated according to the theory of thermionic emission (Sze & Kwok, 2007).

3.4 Boundary parameter (back/front contact to semiconductor boundary models)

The boundaries of the semiconductor stack may either be metallic (usually constituting the contacts of the solar cell) or they may be insulating in order to simulate some specific measurements requiring insulator contacts. Four different boundary models can be chosen: (1) flatband metal/semiconductor contact, (2) Schottky metal/semiconductor contact, (3) insulator contact, (4) metal/insulator/semiconductor contact. If choosing the flatband metal/semiconductor contact, there will be no band banding induced within the semiconductor due to the contact (flatband contact). The electron/hole surface recombination velocities $S_n^{front/back}$, $S_p^{front/back}$ of the metallic contact have to be specified (Sze & Kwok, 2007). If choosing the Schottky metal/semiconductor contact, an additional work function $\phi^{front/back}$ of the metal contact has to be specified. A depletion or accumulation layer within the semiconductor due to the contact will then form according to Schottky theory (Sze & Kwok, 2007). If choosing the insulator/semiconductor or the metal/insulator/semiconductor contact, interface states between the insulator and the semiconductor can be stated, that is an interface defect distribution $N_{trap}^{it}(E)$ and interface capture cross sections σ_n^{it} , σ_p^{it} have to be specified (Kronik & Shapira, 1999). In case of the metal/insulator/semiconductor contact an additional interface capacity $C^{front/back}$ has to be specified (Kronik & Shapira, 1999). Due to the interface defects a band bending within the semiconductor can form.

3.5 Circuit elements

A series resistance R_s , a parallel resistance R_p , a parallel capacitance C_p and in case of an metal/insulator/semiconductor contact also a series capacitance C_s can be specified. If circuit elements are specified, the internal cell voltage V_{int} and the internal cell current I_{int} of the semiconductor stack will differ from the external cell voltage V_{ext} and external cell current I_{ext} of the modeled device.

3.6 External parameters

External parameters are defined to be parameters which are externally applied to the device under consideration and which can also be easily varied in a real experiment. These are the temperature T of the device, a spectral and a monochromatic illumination source leading to the spectral photon flux $\Phi_0(\lambda,t)$ required for the optical simulations, and the external cell voltage $V_{ext}(t)$ or the external cell current $I_{ext}(t)$ which is applied to the device. The remaining quantity, i.e. the external cell current $I_{ext}(t)$ or the external cell voltage $V_{ext}(t)$ respectively, will be calculated.

4. Mathematical description of the DGL system solved by AFORS-HET

In the following, the differential equations and corresponding boundary conditions, which are solved by AFORS-HET under the various conditions, are stated.

An arbitrary stack of semiconductor layers can be modeled. Within each semiconductor layer the Poisson equation and the transport and continuity equations for electrons and holes have to be solved. At each semiconductor/semiconductor interface and at the front and back side boundary of the stack the current transport through these interfaces/boundaries can be described by different physical models. It results a highly non-linear coupled system of three differential equations with respect to time and space derivatives. The electron density $n(x,t)$, the hole density $p(x,t)$, and the electric potential $\varphi(x,t)$ are the independent variables, for which this system of differential equations is solved. It is solved according to the numerical discretisation scheme as outlined by Selberherr (Selberherr, 1984) in order to linearize the problem and using the linear SparLin solver which is available in the internet (Kundert et. al., 1988).
It can be solved for different calculation modes: (1) EQ calculation mode, describing thermodynamic equilibrium at a given temperature, (2) DC calculation mode, describing steady-state conditions under an external applied voltage or current and/or illumination, (3) AC calculation mode, describing small additional sinusoidal modulations of the external applied voltage/illumination, and (4) TR calculation mode, describing transient changes of the system, due to general time dependent changes of the external applied voltage or current and/or illumination.
In case of using the EQ or the DC calculation mode, all time derivatives vanish, resulting in a simplified system of differential equations. The system of differential equations is then solved for the time independent, but position dependent functions, $n^{EQ/DC}(x)$, $p^{EQ/DC}(x)$, $\varphi^{EQ/DC}(x)$.

$$n(x,t) = n^{EQ}(x), \qquad n(x,t) = n^{DC}(x)$$

$$p(x,t) = p^{EQ}(x) \qquad p(x,t) = p^{DC}(x)$$

$$\varphi(x,t) = \varphi^{EQ}(x) \qquad \varphi(x,t) = \varphi^{DC}(x)$$

In case of using the AC calculation mode, it is assumed that all time dependencies can be described by small additional sinusoidal modulations of the steady-state solutions. All time dependent quantities are then modelled with complex numbers (marked by a dash ~), which allows to determine the amplitudes and the phase shifts between them. I.e., for the independent variables of the system of differential equations, one gets:

$$n(x,t) = n^{DC}(x) + \tilde{n}^{AC}(x)\, e^{i\omega t}$$

$$p(x,t) = p^{DC}(x) + \tilde{p}^{AC}(x)\, e^{i\omega t}$$

$$\varphi(x,t) = \varphi^{DC}(x) + \tilde{\varphi}^{AC}(x)\, e^{i\omega t}$$

In case of using the TR calculation mode, the description of the system starts with a steady-state (DC-mode) simulation, specifying an external applied voltage or current and/or illumination. An arbitrary evolution in time of the external applied voltage or current and/or illumination can then be specified by loading an appropriate file. Then, the time evolution of the system, i.e. the functions $n(x,t)$, $p(x,t)$, $\varphi(x,t)$ during and after the externally applied changes are calculated.

4.1 Optical calculation: super bandgap generation models

In order to describe the generation rate $G_n(x,t)$, $G_p(x,t)$ of electrons and holes due to photon absorption within the bulk of the semiconductor layers, a distinction between super-bandgap generation (for photons with an energy $E_{photon} = hc/\lambda \geq E_g$) and sub-bandgap generation (for photons with an energy $E_{photon} = hc/\lambda \leq E_g$) is made ($\lambda$: photon wavelength h: Planck´s constant, c: velocity of light, E_g: bandgap of the semiconductor layer in which the photon absorption takes place). Only the super-bandgap generation rate is calculated by optical modelling as it is independent of the local particle densities $n(x,t)$, $p(x,t)$. Sub-bandgap generation depends on the local particle densities and must therefore be calculated within the electrical modeling part.

The optical super-bandgap generation rate is equal for electrons and holes $G(x,t) = G_n(x,t) = G_p(x,t)$. It can either be imported by loading an appropriate file (using external programs for its calculation) or it can be calculated within AFORS-HET.

So far, two optical models are implemented in AFORS-HET, i.e. the optical model Lambert-Beer absorption and the optical model coherent/incoherent internal multiple reflections. The first one takes textured surfaces and multiple internal boundary reflections into account (due to simple geometrical optics) but neglects coherence effects. It is especially suited to treat wafer based crystalline silicon solar cells. The second takes coherence effects into account, but this is done only for plain surfaces. If coherence effects in thin film solar cells are observable it may be used.

4.1.1 Optical model: Lambert-Beer absorption

Using this model, the absorption within the semiconductor stack will be calculated assuming simple Lambert-Beer absorption, allowing for multiple for and backward traveling of the incoming light, however disregarding coherent interference. A (measured) reflectance and absorptance file of the illuminated contact $R(\lambda)$, $A(\lambda)$ can be loaded or constant values can be used. The incoming spectral photon flux $\Phi_0(\lambda,t)$ is weighted with the contact reflection and absorption, i.e. the photon flux impinging on the first semiconductor layer is given by $\Phi_0(\lambda,t)R(\lambda)A(\lambda)$. To simulate the extended path length caused by a textured surface, the angle of incidence δ of the incoming light can be adjusted. On a textured Si wafer with <111> pyramids, this angle is δ=54.74°, whereas δ=0° equals normal incidence. The angle γ in which the light travels through the layer stack depends on the wavelength of the incoming light and is calculated according to Snellius' law:

$$\gamma(\lambda) = \delta - \arcsin\left\{\sin(\delta)\cdot\frac{1}{n(\lambda)}\right\},$$

whereas $n(\lambda)$ is the wavelength dependent refraction index of the first semiconductor layer at the illuminated side. Note, that within this model, the change in $\gamma(\lambda)$ is neglected, when the light passes a semiconductor/semiconductor layer interface with two different refraction indices. Thus it is assumed that all photons with a specified wavelength cross the layer stack under a distinct angle γ.

Photon absorption is then calculated from the spectral absorption coefficient $\alpha_x(\lambda) = 4\pi\, k(\lambda)/\lambda$ of the semiconductor layer corresponding to the position x within the stack, which is calculated from the provided extinction coefficient $k(\lambda)$ of the layer. The

super bandgap electron/hole generation rate for one single run trough the layer stack (no multiple passes) is then given by:

$$G(x,t) = \int_{\lambda_{\min}}^{\lambda_{\max}} d\lambda \; \Phi_0(\lambda,t) R(\lambda) A(\lambda) \; \alpha_x(\lambda) \; e^{\frac{-\alpha_x(\lambda)\, x}{\cos(\gamma)}} .$$

The minimum and maximum wavelengths $\lambda_{\min}$, $\lambda_{\max}$ for the integration are generally provided by the loaded spectral range of the incoming spectral photon flux, $\Phi_0(\lambda,t)$. However, if necessary, $\lambda_{\max}$ is modified in order to ensure that only super-bandgap generation is considered: $\lambda_{\max} \le hc / E_g$.

To simulate the influence of light trapping mechanisms, internal reflections at both contacts can be additionally specified. They can either be set as a constant value or wavelength dependant (a measured or calculated file can be loaded). The light then passes through the layer stack several times as defined by the user, thereby enhancing the absorptivity of the layer stack (the local generation rate). The residual flux after the defined number of passes is added to the transmitted flux at the contact, at which the calculation ended (illuminated or not-illuminated contact), disregarding the internal reflection definitions at this contact.

This model was designed to estimate the influence of light trapping of crystalline silicon solar cells and to adapt the simulation to real measurements. However, it neglects the internal multiple reflections and refractions within the layer stack.

4.1.2 Optical model: coherent/incoherent internal multiple reflections

Using this model, the absorption within the semiconductor stack will be calculated by modelling coherent or incoherent internal multiple reflections within the semiconductor stack. Additional non-conducting optical layers in front of the front contact/behind the back contact of the solar cell can be assumed, for example in order to model the effect of anti-reflection coatings. Normal incidence of the incoming illumination is assumed.

The reflectance, transmittance and absorptance of all layers (optical layers and the semiconductor layers) is calculated, using the concepts of complex Fresnel amplitudes. Each layer can be specified to be optically coherent or optically incoherent for a particular light beam (incident illumination). A layer is considered to be coherent if its thickness is smaller than the coherence length of the light beam that is incident on the system.

In order to be able to consider coherent effects, the specified incoming illumination $\Phi_0(\lambda,t)$ is modeled by an incoming electromagnetic wave, with a complex electric field component $\tilde{E}_0^+(\lambda,t)$ (front side illumination, electromagnetic wave traveling in positive direction towards the back contact, with $\Phi_0(\lambda,t) = Const \left|\tilde{E}_0^+(\lambda,t)\right|^2$), or $\tilde{E}_{N+1}^-(\lambda,t)$ respectively (back side illumination, electromagnetic wave traveling in negative direction towards the front contact, with $\Phi_0(\lambda,t) = Const \left|\tilde{E}_{N+1}^-(\lambda,t)\right|^2$). The complex electric field components of the travelling wave are raytraced according to the Fresnel formulas, and thus the resulting electromagnetic wave $\tilde{E}(x,\lambda,t)$ at any position x within the layer stack is calculated. An incoherent layer is modeled by a coherent calculation of several electromagnetic waves within that layer (specified by the integer $N_{incoherentIterations}$), assuming some phase shift between them, and averaging over the resulting electric field components.

4.2 Electrical calculation - bulk layers: semiconductor bulk models

Within the bulk of each semiconductor layer, Poisson's equation and the transport equations for electrons and holes are to be solved in one dimension. So far, there are two semiconductor bulk models available, i.e. the bulk model "standard semiconductor" and the bulk model "crystalline silicon". If using the standard semiconductor model, all bulk layer input parameters as specified in Chapter 3.2 can be individually adjusted. If using the crystalline silicon bulk model, most input parameters for crystalline silicon are calculated from few remaining input parameters, i.e. from the doping and defect densities $N_D(x)$, $N_A(x)$, N_{trap} of crystalline silicon. Thus effects like band gap narrowing or the doping dependence of the mobility or of the Auger recombination of crystalline silicon are explicitly modeled.

Within each layer, a functional dependence in space can be specified for the doping densities $N_D(x)$, $N_A(x)$. These input parameters can be chosen to be (1) constant, (2) linear, (3) exponential, (4) Gaussian like, (5) error function like decreasing or increasing as a function of the space coordinate x.

4.2.1 Bulk model: standard semiconductor

The doping densities $N_D(x)$, $N_A(x)$ of fixed donator/acceptor states at apposition x within the cell are assumed to be always completely ionized. Contrary, defects $N_{trap}(E)$ located at a specific energy E within the bandgap of the semiconductor can be locally charged/uncharged within the system. Defects can be chosen to be either (1) acceptor-like Shockley-Read-Hall defects, (2) donor-like Shockley-Read-Hall defects or (3) dangling bond defects. Depending on the defect-type chosen, these defects can either be empty, singly occupied with electrons or even doubly occupied with electrons (in case of the dangling bond defect). Acceptor-like Shockley-Read-Hall defects are negatively charged, if occupied and neutral, if empty. Donor-like Shockley-Read-Hall defects are positively charged, if empty, and neutral, if occupied. Dangling bond defects are positively charged, if empty, neutral, if singly occupied and negatively charged, if doubly occupied.

Poisson´s equation, which is to be solved within each layer, reads:

$$\frac{\varepsilon_0 \varepsilon_r}{q} \frac{\partial^2 \varphi(x,t)}{\partial x^2} = p(x,t) - n(x,t) + N_D(x) - N_A(x) + \sum_{trap} \rho_{trap}(x,t)$$

q being the electron charge and ε_0, ε_r being the absolute/relative dielectric constant. The defect density of charged defects $\rho_{trap}(x,t)$ will depend on the defect-type of the defect under consideration and on the local particle densities $n(x,t), p(x,t)$ within in the system. It is described by a trap density distribution function $N_{trap}(E)$ of the defect, specifying the amount of traps at an energy position E within the bandgap and by some corresponding defect occupation functions $f^{SRH}_{0,trap}(E,x,t)$, $f^{SRH}_{1,trap}(E,x,t)$, $f^{DB}_{+,trap}(E,x,t)$, $f^{DB}_{0,trap}(E,x,t)$, $f^{DB}_{-,trap}(E,x,t)$, specifying the probability that traps with an energy position E within the bandgap are empty or singly or doubly occupied with electrons. Thus $\rho_{trap}(x,t)$ equates to $\rho_{trap}(x,t) = -\int dE \; f^{SRH}_{1,trap}(E,x,t) \; N_{trap}(E)$ in case of acceptor-like Shockley-Read-Hall defects, $\rho_{trap}(x,t) = +\int dE \; f^{\mathrm{SRH}}_{0,trap}(E,x,t) \; N_{trap}(E)$ in case of donator-like Shockley-Read-Hall defects, $\rho_{trap}(x,t) = +\int dE \; \left(f^{\mathrm{DB}}_{+,trap}(E,x,t) - f^{\mathrm{DB}}_{-,trap}(E,x,t)\right) N_{trap}(E)$ in case of dangling bond defects.

The explicit formulas for the defect occupation functions $f_{0,trap}^{SRH}(E,x,t)$, $f_{1,trap}^{SRH}(E,x,t)$, $f_{+,trap}^{DB}(E,x,t)$, $f_{0,trap}^{DB}(E,x,t)$, $f_{-,trap}^{DB}(E,x,t)$ are described later within this text.

The one dimensional equations of continuity and transport for electrons and holes, which have to be solved within each layer, read:

$$-\frac{1}{q}\frac{\partial j_n(x,t)}{\partial x} = G_n(x,t) - R_n(x,t) \; - \frac{\partial}{\partial t} n(x,t)$$

$$+\frac{1}{q}\frac{\partial j_p(x,t)}{\partial x} = G_p(x,t) - R_p(x,t) \; - \frac{\partial}{\partial t} p(x,t)$$

The electron/hole super-bandgap generation rates $G_n(x,t)$, $G_p(x,t)$ have to be determined by optical modeling, the corresponding recombination rates $R_n(x,t)$, $R_p(x,t)$ are described later in this text. The electron/hole currents $j_n(x,t)$, $j_p(x,t)$ are driven by the gradient of the corresponding quasi Fermi energy $E_{Fn}(x,t)$, $E_{Fp}(x,t)$. Using a Maxwell Boltzmann approximation for the Fermi-Dirac distribution function, the position dependent Fermi energies and the corresponding local electron/hole currents are explicitly:

$$E_{Fn}(x,t) = E_C(x) + kT \ln\frac{n(x,t)}{N_C(x)} = -q\chi(x) + q\varphi(x,t) + kT \ln\frac{n(x,t)}{N_C(x)}$$

$$E_{Fp}(x,t) = E_V(x) - kT \ln\frac{p(x,t)}{N_V(x)} = -q\chi(x) + q\varphi(x,t) - E_g(x) - kT \ln\frac{p(x,t)}{N_V(x)}$$

$$j_n(x,t) = q\,\mu_n\, n(x,t)\, \frac{\partial E_{Fn}(x,t)}{\partial x}$$

$$j_p(x,t) = q\,\mu_p\, p(x,t)\, \frac{\partial E_{Fp}(x,t)}{\partial x}$$

with the corresponding electron/hole mobilities μ_n, μ_p, the electron affinity χ, the bandgap E_g, the conduction/valence band energy E_C, E_V and the effective conduction/valence band density of states N_C, N_V of the semiconductor.

Recombination

Recombination from the conduction band into the valence band may occur directly, i.e. via radiative band to band recombination, $R_{n,p}^{BB}(x,t)$, or via Auger recombination, $R_{n,p}^{A}(x,t)$. It may also occur via defect states located within the bandgap of the semiconductor, i.e. via Shockley-Read-Hall recombination $R_{n,p}^{SHR}(x,t)$ or via dangling bond recombination, $R_{n,p}^{DB}(x,t)$:

$$R_{n,p}(x,t) = R_{n,p}^{BB}(x,t) + R_{n,p}^{A}(x,t) + R_{n,p}^{SHR}(x,t) + R_{n,p}^{DB}(x,t)$$

Optical sub-bandgap generation

Optical sub-bandgap generation (for $hc/\lambda < E_g$) is calculated using Shockley-Read-Hall recombination statistics. A negative electron/hole SHR recombination rate $R_n^{SRH}(x,t)$,

$R_p^{SRH}(x,t)$ means sub-bandgap generation of an electron/hole from a defect state (trap) into the conduction/valence band. Sub-bandgap generation can either be voltage driven and/or be driven by an optical excitation.

The SRH optical emission coefficients $e_{n,optical}^{trap}(E,x,t)$, $e_{p,optical}^{trap}(E,x,t)$ can be calculated from the optical electron/hole capture cross sections $\sigma_{n,optical}^{trap}$, $\sigma_{p,optical}^{trap}$:

$$e_{n,optical}^{trap}(E,x,t) = \int_{\lambda_{\min}}^{\lambda_{\max}} d\lambda \;\; \sigma_{n,optical}^{trap} \; N_C \; \Phi(\lambda,x,t) \; \vartheta(E_C - E - hc/\lambda)$$

$$e_{p,optical}^{trap}(E,x,t) = \int_{\lambda_{\min}}^{\lambda_{\max}} d\lambda \;\; \sigma_{p,optical}^{trap} \; N_V \; \Phi(\lambda,x,t) \; \vartheta(E - E_V - hc/\lambda)$$

with $\Phi(\lambda,x,t)$: spectral photon flux inside the semiconductor layers, of wavelength λ at the position x and at time t, N_C, N_V: effective conduction/valence band density, E_C, E_V: energy position of the conduction/valence band, and $\vartheta(E)$: step function, $\vartheta(E) = 1 \; for \; E \le 0$, $\vartheta(E) = 0 \; for \; E > 0$.

Again, the minimum and maximum wavelengths $\lambda_{\min}$, $\lambda_{\max}$ for the integration are generally provided by the loaded spectral range of the incoming spectral photon flux, $\Phi_0(\lambda,t)$. However, if necessary, $\lambda_{\min}$ is modified in order to ensure that only sub-bandgap generation is considered: $\lambda_{\min} \ge hc/E_g$.

Radiative recombination

The radiative band to band rate constant r^{BB} has to be specified in order to equate the radiative band to band recombination rates $R_{n,p}^{BB}(x,t)$. The resulting electron and hole recombination rates are always equal:

$$R_{n,p}^{BB}(x,t) = r^{BB} \; \left\{ n(x,t)\, p(x,t) - N_C \; N_V \; e^{-E_g/kT} \right\}$$

In case of using the DC or AC calculation mode and neglecting second order terms in case of the AC calculation mode, this simplifies to

$$R_{n,p}^{BB}(x) = r^{BB} \; \left\{ n^{DC}(x)\, p^{DC}(x) - N_C \; N_V \; e^{-E_g/kT} \right\}$$

$$R_{n,p}^{BB}(x,t) = R_{n,p}^{BB}(x) + \tilde{R}_{n,p}^{BB}(x) \; e^{i\omega t}$$

$$\tilde{R}_{n,p}^{BB}(x) = r^{BB} \; n^{DC}(x) \; \tilde{p}^{AC}(x) + r^{BB} \, p^{DC}(\mathrm{x}) \; \tilde{n}^{AC}(x)$$

Auger recombination

The electron/hole Auger rate constants r_n^A, r_p^A have to be specified in order to calculate the Auger recombination rates $R_{n,p}^{A}(x,t)$. Again, the resulting electron and hole recombination rates are always equal:

$$R_{n,p}^{A}(x,t) = \left[r_n^A \; n(x,t) + r_p^A \; p(x,t) \right] \; \left\{ n(x,t)\, p(x,t) - N_C \; N_V \; e^{-E_g/kT} \right\}$$

In case of using the DC or AC calculation mode, neglecting second order terms within the AC calculation mode, this simplifies to

$$R^A_{n,p}(x) = \left[r_n^A\, n^{DC}(x) + r_p^A\, p^{DC}(x)\right] \left\{ n^{DC}(x)\, p^{DC}(x) - N_C\, N_V\, e^{-E_g/kT} \right\}$$

$$R^A_{n,p}(x,t) = R^A_{n,p}(x) + \tilde{R}^A_{n,p}(x)\, e^{i\omega t}$$

$$\tilde{R}^A_{n,p}(x) = \left[r_n^A\, n^{DC}(x)^2 + 2\, r_p^A\, n^{DC}(x)\, p^{DC}(x)\right] \tilde{p}^{AC}(x) + \left[r_p^A\, p^{DC}(x)^2 + 2\, r_n^A\, n^{DC}(x)\, p^{DC}(x)\right] \tilde{n}^{AC}(x)$$

Shockley Read Hall recombination

Shockley-Read-Hall recombination (Shockley & Read, 1952) requires specifying the character (acceptor-like or donor-like), the capture cross sections σ_n^{trap}, σ_p^{trap}, $\sigma_{n,optic}^{trap}$, $\sigma_{p,optic}^{trap}$ and the energetic distribution $N_{trap}(E)$ of the defect density within the bandgap of the semiconductor, of each defect. An arbitrary number of defects with either one of the following energetic distributions $N_{trap}(E)$ can be chosen:

1. point like distributed at a single energy E_{trap} within the bandgap:

   $$N_{trap}(E) = N_{trap}^{point}\, \delta(E - E_{trap})$$

   with N_{trap}^{point}: defect density of the point like defect, $\delta(E)$: delta function
2. constantly distributed within a specific region within the bandgap:

   $$N_{trap}(E) = \left(E_{trap}^{end} - E_{trap}^{start}\right) N_{trap}^{const}\, \vartheta(E - E_{trap}^{end})\, \vartheta(E_{trap}^{start} - E)$$

   with E_{trap}^{start}, E_{trap}^{end}: start and end energy of the energy interval within the bandgap, where a constant defect density is assumed, N_{trap}^{const}: constant defect density per energy, $\vartheta(E)$: step function
3. exponentially decaying from the conduction/valence band into the bandgap:

   $$N_{trap}(E) = N_{trap}^{C,tail}\, e^{-(E_C - E)/E_{trap}^{C,tail}},\ N_{trap}(E) = N_{trap}^{V,tail}\, e^{-(E - E_V)/E_{trap}^{V,tail}}$$

   i.e. conduction/valence band tail states, with $N_{trap}^{C,tail}$, $N_{trap}^{V,tail}$: tail state density per energy at the conduction/valence band, $E_{trap}^{C,tail}$, $E_{trap}^{V,tail}$: characteristic decay energy (Urbach energy) of the conduction/valence band tail state,
4. Gaussian distributed within the bandgap:

   $$N_{trap}(E) = \frac{N_{trap}^{db}}{\sigma_{trap}^{db}\sqrt{2\pi}}\, e^{-\frac{\left(E - E_{trap}^{db}\right)^2}{2\sigma_{trap}^{db\,2}}}$$

   i.e. dangling bond states, with N_{trap}^{db}: total dangling bond state density, E_{trap}^{db}: specific energy of the Gaussian dangling bond peak, σ_{trap}^{db}: standard deviation of the Gaussian dangling bond distribution.

For each defect, electron/hole capture coefficients $c_{n,p}^{trap}$ are equated

$$c_{n,p}^{trap} = v_{n,p}\ \sigma_{n,p}$$

with $v_{n,p}$: electron/hole thermal velocity, $\sigma_{n,p}$: electron/hole capture cross section of the defect. The corresponding electron/hole emission coefficients $e_{n,p}^{trap}(E,x,t)$ are then given by:

$$e_n^{trap}(E,x,t) = c_n^{trap}\ N_C\ e^{-(E_C-E)/kT} + e_{n,optic}^{trap}(E,x,t)$$

$$e_p^{trap}(E,x,t) = c_p^{trap}\ N_V\ e^{-(E-E_V)/kT} + e_{p,optic}^{trap}(E,x,t)$$

In case of using the DC or AC calculation mode, this simplifies to

$$e_n^{trap}(E,x) = c_n^{trap}\ N_C\ e^{-(E_C-E)/kT} + \int d\lambda\ \sigma_{n,optic}^{trap}\ N_C\ \Phi(\lambda,x)\ \vartheta(E_C - E - hc/\lambda) \quad \text{(DC mode)}$$

$$e_p^{trap}(E,x) = c_p^{trap}\ N_V\ e^{-(E-E_V)/kT} + \int d\lambda\ \sigma_{p,optic}^{trap}\ N_V\ \Phi(\lambda,x)\ \vartheta(E - E_V - hc/\lambda)$$

$$e_{n,p}^{trap}(E,x,t) = e_{n,p}^{trap}(E,x) + \tilde{e}_{n,p}^{trap}(E,x)\ e^{i\omega t} \quad \text{(AC mode)}$$

$$\tilde{e}_n^{trap}(E,x) = \int d\lambda\ \sigma_{n,optic}^{trap}\ N_C\ \tilde{\Phi}(\lambda,x)\ \vartheta(E_C - E - hc/\lambda)$$

$$\tilde{e}_p^{trap}(E,x) = \int d\lambda\ \sigma_{p,optic}^{trap}\ N_V\ \tilde{\Phi}(\lambda,x)\ \vartheta(E - E_V - hc/\lambda)$$

Finally, the Shockley-Read-Hall recombination rate due to the defects is

$$R_n^{SRH}(x,t) = \sum_{trap} \int dE \left\{ c_n^{trap}\ n(x,t) N_{trap}(E)\ f_{0,trap}^{SRH}(E,x,t) - e_n^{trap}(E,x,t) N_{trap}(E)\ f_{1,trap}^{SRH}(E,x,t) \right\}$$

$$R_p^{SRH}(x,t) = \sum_{trap} \int dE \left\{ c_p^{trap}\ p(x,t) N_{trap}(E)\ f_{1,trap}^{SRH}(E,x,t) - e_p^{trap}(E,x,t) N_{trap}(E)\ f_{0,trap}^{SRH}(E,x,t) \right\}$$

In case of using the DC or AC calculation mode, neglecting second order terms and assuming zero optical emission coefficients within the AC calculation mode (actual stage of the AFORS-HET development at the moment) this simplifies to

$$R_n^{SRH}(x) = \sum_{trap} \int dE \left\{ c_n^{trap}\ n^{DC}(x) N_{trap}(E)\ f_{0,trap}^{SRH}(E,x) - e_n^{trap}(E,x) N_{trap}(E)\ f_{1,trap}^{SRH}(E,x) \right\}$$

$$R_p^{SRH}(x) = \sum_{trap} \int dE \left\{ c_p^{trap}\ p^{DC}(x) N_{trap}(E)\ f_{1,trap}^{SRH}(E,x) - e_p^{trap}(E,x) N_{trap}(E)\ f_{0,trap}^{SRH}(E,x) \right\}$$

$$R_{n,p}^{SRH}(x,t) = R_{n,p}^{SRH}(x) + \tilde{R}_{n,p}^{SRH}(x) e^{i\omega t}$$

$$\tilde{R}_n^{SRH}(x) = \sum_{trap} \int dE \left\{ c_n^{trap}\ N_{trap}(E)\ f_{0,trap}^{SRH}(E,x)\ \tilde{n}^{AC}(x) - \left(c_n^{trap} + e_n^{trap}(E,x)\right) N_{trap}(E)\ \tilde{f}_{1,trap}^{SRH}(E,x) \right\}$$

$$\tilde{R}_p^{SRH}(x) = \sum_{trap} \int dE \left\{ c_p^{trap}\ N_{trap}(E)\ f_{1,trap}^{SRH}(E,x)\ \tilde{p}^{AC}(x) + \left(c_p^{trap} + e_p^{trap}(E,x)\right) N_{trap}(E)\ \tilde{f}_{1,trap}^{SRH}(E,x) \right\}$$

A positive electron/hole SHR recombination rate means recombination of an electron/hole from the conduction/valence band into the defect state (trap), a negative electron/hole SHR recombination rate means sub-bandgap generation of an electron/hole from the defect state (trap) into the conduction/valence band.

Dangling bond recombination

To calculate charge state and recombination of dangling bond defects in amorphous silicon the most exact description developed by Sah and Shockley (Sah & Shockley, 1958) is used. Three different occupation functions $f^{DB}_{+,trap}(E,x,t)$, $f^{DB}_{0,trap}(E,x,t)$, $f^{DB}_{-,trap}(E,x,t)$ for the positively, neutral and negatively charge states have to be derived, corresponding to the empty, single or double occupied electronic state. Four capture/emission processes with the capture cross sections σ_n^+, σ_p^0, σ_n^0, σ_p^- have to be defined as can be seen in Fig. 3. The two transition energies $E_{0/-}$, $E_{+/0}$ are separated by the correlation energy U, which accounts for the fact that the capture-emission process is influenced by the charge state of the dangling or by rearrangement of the lattice in the surrounding.

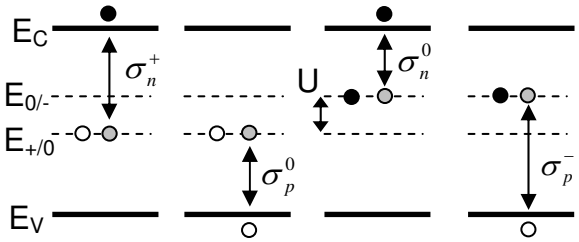

Fig. 3. dangling bond recombination according to Sah and Shockley

For each defect, electron/hole capture coefficients $c^{trap}_{n/p,+/0/-}$ are calculated with the specified electron/hole thermal velocity $v_{n/p}$:

$$c^{trap}_{n/p,+/0/-} = v_{n/p}\,\sigma^{+/0/-}_{n/p}$$

The emission coefficients for the DC calculation mode, neglecting optical emission are given by:

$$e^{trap}_{n,0}(E,x) = \frac{1}{2} c^{trap}_{n,+}\, N_C\, e^{-(E_C-E)/kT}$$

$$e^{trap}_{p,+}(E,x) = 2c^{trap}_{p,0}\, N_V\, e^{-(E-E_V)/kT}$$

$$e^{trap}_{n,-}(E,x) = 2c^{trap}_{n,0}\, N_C\, e^{-(E_C-(E+U))/kT}$$

$$e^{trap}_{p,0}(E,x) = \frac{1}{2} c^{trap}_{p,-}\, N_V\, e^{-(E+U-E_V)/kT}$$

Finally the dangling bond recombination coefficients are given by:

$$R^{DB}_n(x) = \sum_{trap} \int dE \left\{ c^{trap}_{n,+}\, n^{DC}(x) N_{trap}(E)\, f^{DB}_{+,trap}(E,x) - e^{trap}_{n,0}(E,x) N_{trap}(E) f^{DB}_{0,trap}(E,x) + c^{trap}_{n,0}\, n^{DC}(x) N_{trap}(E)\, f^{DB}_{0,trap}(E,x) - e^{trap}_{n,-}(E,x) N_{trap}(E) f^{DB}_{-,trap}(E,x) \right\}$$

$$R_p^{DB}(x) = \sum_{trap} \int dE \left\{ c_{p,-}^{trap}\ p^{DC}(x) N_{trap}(E)\ f_{-,trap}^{DB}(E,x) - e_{p,0}^{trap}(E,x) N_{trap}(E) f_{0,trap}^{DB}(E,x) + \right.$$
$$\left. c_{p,0}^{trap}\ p^{DC}(x) N_{trap}(E)\ f_{0,trap}^{DB}(E,x) - e_{p,+}^{trap}(E,x) N_{trap}(E) f_{+,trap}^{DB}(E,x) \right\}$$

Dangling bond recombination is still under development. Especially time dependent recombination and optical defect to band emissions are not implemented at the current state of AFORS-HET development.

Defect occupation functions

The defect occupation functions $f_{0,trap}^{SRH}(E,x,t)$, $f_{1,trap}^{SRH}(E,x,t)$, $f_{+,trap}^{DB}(E,x,t)$, $f_{0,trap}^{DB}(E,x,t)$, $f_{-,trap}^{DB}(E,x,t)$ specify the probability for a specific defect (either Shockley-Read-Hall or dangling bond) that traps with an energy position E within the bandgap of the semiconductor are empty or singly or even doubly occupied with electrons.
In case of using the DC or AC calculation mode, they can be explicitly expressed in terms of the local particle densities $n^{DC}(x)$, $p^{DC}(x)$, $\tilde{n}^{AC}(x)$, $\tilde{p}^{AC}(x)$. In case of using the TR calculation mode, the defect occupation functions are generally determined by additional differential equations. Transient DB defect occupation functions have not been implemented in AFORS-HET yet (actual stage of AFORS-HET development).

Shockley Read Hall defect occupation functions

A Shockley-Read-Hall defect can be either empty or occupied by an electron, thus

$$f_{0,trap}^{SRH}(E,x,t) + f_{1,trap}^{SRH}(E,x,t) = 1$$

The Shockley-Read-Hall defect occupation function $f_{1,trap}^{SRH}(E,x,t)$ for electrons will be explicitly stated in case of using the EQ, DC, AC or the TR calculation mode. The Shockley-Read-Hall defect occupation function $f_{0,trap}^{SRH}(E,x,t)$ can then directly be equated.
Generally, a local change of the trapped charge stored in SRH defects must be determined by the difference between the local electron and hole SRH recombination rates:

$$\frac{d}{dt}\rho_{\text{trap}}(x,t) = R_p^{SHR}(x,t) - R_n^{SHR}(x,t)$$

This defines for each defect an additional differential equation for its SHR defect occupation function $f_{1,trap}^{SRH}(E,x,t)$ with respect to its time derivative:

$$\frac{d}{dt} f_{1,trap}^{SRH}(E,x,t) = \left(c_n^{trap}\ n(x,t) + e_p^{trap}(E,x,t)\right)\left(1 - f_{1,trap}^{SRH}(E,x,t)\right) - \left(c_p^{trap}\ p(x,t) + e_n^{trap}(E,x,t)\right) f_{1,trap}^{SRH}(E,x,t) \quad (\#)$$

In case of using the EQ or the DC calculation mode, the time derivative vanishes, and an explicit expression for the SHR defect occupation function, $f_{1,trap}^{SRH,DC}(E,x)$, which is no longer time dependant, can be derived:

$$f_{1,trap}^{SRH,DC}(E,x) = \frac{c_n^{trap}\ n^{DC}(x) + e_p^{trap}(E,x)}{c_n^{trap}\ n^{DC}(x) + e_n^{trap}(E,x) + c_p^{trap}\ p^{DC}(x) + e_p^{trap}(E,x)}$$

Of course, in case of using the EQ calculation mode, the SHR defect occupation function could be also equivalently be described by the Fermi-Dirac distribution function, $f_{1,\,trap}^{SRH,DC}(E,x) = f_{1,\,trap}^{SRH,EQ}(E,x)$, which implicitly determines the position independent Fermi energy E_F.

$$f_{1,\,trap}^{SRH,EQ}(E,x) = \frac{1}{1+e^{\frac{E-E_F}{kT}}}$$

In case of using the AC calculation mode, the differential equation (#) can be explicitly solved, assuming time independent optical emission coefficients within the AC calculation mode (actual stage of the AFORS-HET development at the moment) and assuming the time dependencies $n(x,t) = n^{DC}(x) + \tilde{n}^{AC}(x)\, e^{i\omega t}$, $p(x,t) = p^{DC}(x) + \tilde{p}^{AC}(x)\, e^{i\omega t}$. Neglecting second order terms, one gets for the SHR defect occupation function in the AC calculation mode, $f_{1,\,trap}^{SRH,AC}(E,x,t)$:

$$f_{1,\,trap}^{SRH,AC}(E,x,t) = f_{1,\,trap}^{SRH,DC}(E,x) + \tilde{f}_{1,\,trap}^{SRH,AC}(E,x)\, e^{i\omega t}$$

$$\tilde{f}_{1,\,trap}^{SRH,AC}(E,x) = \frac{c_n^{trap}\, f_{0,\,trap}^{SRH,DC}(E,x)\, \tilde{n}^{AC}(x) \;-\; c_p^{trap}\, f_{1,\,trap}^{SRH,DC}(E,x)\, \tilde{p}^{AC}(x)}{c_n^{trap}\, n^{DC}(x) + e_n^{trap}(E,x) + c_p^{trap}\, p^{DC}(x) + e_p^{trap}(E,x) + i\omega}$$

In case of using the TR calculation mode, the transient SRH defect occupation function $f_{1,\,trap}^{SRH,TR}(E,x,t_{i+1})$ at the time step t_{i+1} for an evolution of the system from the time point t_i towards the time point t_{i+1} can be stated by solving the differential equation (#) using a full implicit time discretisation scheme with respect to the particle densities and the emission rates:

$$\begin{aligned}&\frac{d}{dt} f_{1,\,trap}^{SRH,TR}(E,x,t)\\ &= \left(c_n^{trap}\, n(x,t_{i+1}) + e_p^{trap}(E,x,t_{i+1})\right)\left(1 - f_{1,\,trap}^{SRH,TR}(E,x,t)\right) - \left(c_p^{trap}\, p(x,t_{i+1}) + e_n^{trap}(E,x,t_{i+1})\right) f_{1,\,trap}^{SRH,TR}(E,x,t)\end{aligned}$$

An analytical solution of this differential equation leads to:

$$f_{1,\,trap}^{SRH,TR}(E,x,t_{i+1}) = f_{1,\,trap}^{SRH,DCtr}(E,x,t_{i+1}) - \frac{f_{1,\,trap}^{SRH,DCtr}(E,x,t_{i+1}) - f_{1,\,trap}^{SRH,TR}(E,x,t_i)}{e^{dt\,\left(c_n^{trap}\, n(x,t_{i+1}) + e_n^{trap}(E,x,t_{i+1}) + c_p^{trap}\, p(x,t_{i+1}) + e_p(E,x,t_{i+1})\right)}}$$

with

$$f_{SRH}^{DCtr}(E,x,t_{i+1}) = \frac{c_n^{trap}\, n(x,t_{i+1}) + e_p^{trap}(E,x,t_{i+1})}{c_n^{trap}\, n(x,t_{i+1}) + e_n^{trap}(E,x,t_{i+1}) + c_p^{trap}\, p(x,t_{i+1}) + e_p^{trap}(E,x,t_{i+1})}$$

In the steady-state limit, i.e. for Limes $dt \to \infty$, $dt = t_{i+1} - t_i$, this formula converts to the well known steady state SRH defect occupation function $f_{1,\,trap}^{SRH,DC}(E,x) = f_{1,\,trap}^{SRH,DCtr}(E,x,t_{i+1})$.

Dangling bond defect occupation functions

A dangling bond defect can be either empty or singly or doubly occupied by an electron, hereby being in its positive, neutral or negative charged state, thus